Core cross-linked polymeric micelles based on polypept(o)ides: from secondary structure formation of polypeptides to functional cross-linking strategies for polymeric micelles

Bauer, T.A.

Racemic S-(Ethylsulfonyl)-DL-N-carboxyanhydrides Improve Chain Lengths and Monomer Conversion for β-Sheet Controlled Ring-Opening Polymerization

Racemic *S*-(Ethylsulfonyl)-DL-*N*-carboxyanhydrides Improve Chain Lengths and Monomer Conversion for β-Sheet Controlled Ring-Opening Polymerization

Tobias A. Bauer[a, b], Christian Muhl[b], Dieter Schollmeyer[b], Matthias Barz[a, b,*]

[a] Leiden Academic Centre for Drug Research (LACDR), Leiden University, Einsteinweg 55, 2333 CC Leiden, The Netherlands

[b] Department of Chemistry, Johannes Gutenberg University Mainz, Duesbergweg 10-14, 55128 Mainz, Germany

Abstract

The secondary structure formation of polypeptides not only governs folding and solution self-assembly but affects the nucleophilic ring-opening polymerization of α-amino acid-*N*-carboxyanhydrides (NCAs). Whereby helical structures are known to enhance polymerization rates, ß-sheet-like assemblies reduce the propagation rate or may even terminate chain growth by precipitation or gelation. To overcome these unfavorable properties, racemic mixtures of NCAs can be applied. In this work, racemic *S*-(ethylsulfonyl)-DL-cysteine NCA is investigated for the synthesis of polypeptides, diblock and triblock copolypept(o)ides. In contrast to the polymerization of stereoregular *S*-(ethylsulfonyl)-L-cysteine NCA, the reaction of *S*-(ethylsulfonyl)-DL-cysteine NCA proceeds with a rate constant of up to $k_p = 1.70 \times 10^{-3}$ L·mol^{-1}·s^{-1} and is slightly faster than the enatiopure polymerization. While the polymerization of *S*-(ethylsulfonyl)-L-cysteine NCA suffers from incomplete monomer conversion and DPs limited to 30 - 40, racemic mixtures yield polypeptides with DPs of up to 102 with high conversion rates and well-defined dispersities (1.2 - 1.3). The controlled living nature of the ring-opening polymerization of *S*-(ethylsulfonyl)-DL-cysteine NCA thus enables the synthesis of triblock copolymers by sequential monomer addition. This methodology allows for precise control over DPs of individual blocks and yields uniform triblock copolymers with symmetric molecular weight distributions at a reduced synthetic effort.

Keywords

polypept(o)ides · NCA polymerization · ring-opening polymerization · racemic amino acids · polypeptides

Introduction

Ring-opening polymerization (ROP) of *N*-carboxyanhydrides (NCAs) provides easy access to polypeptides, and their use as multi-functional polymeric material.[1–3] Besides properties derived from specific side- or end-groups, polypeptides feature the formation of higher ordered secondary structures, which can be mainly divided into either α-helices or ß-sheets, with exemptions for proline-type amino acids.[4] For controlled living NCA polymerization following the normal amine mechanism, secondary structure formation was shown to have a major impact on the polymerization itself, i.e., reaction kinetics and polypeptide solubility as well as polymer analytics.[1,5–8]

Polymerization of NCAs leading to homopolymers with a high degree of α-helical segments, e.g., *N*-ε-(carbobenzoxy-carbonyl)-L-lysine or γ-(benzyl)-L-glutamate (p(L)Glu(OBn)), starts upon initiation and a short induction period with relatively slow polymerization rate, which is displaced by fast and pseudo-first order kinetics for later stages of the reaction. Early investigations by Lundberg and Doty as well as recent detailed studies by the Cheng group, could explain the increased polymerization rate by an occurring transition from a rather ß-sheet-like structure to an α-helical growth supporting the addition of NCA monomers by directed hydrogen-bonds and an induced dipole.[9–11] In this context, for amino acids forming strong ß-sheets from homo-oligopeptides, NCA polymerization is slowed down and may even stop during the induction period as a result of precipitation or crystallization.[12–15] As such, poly(L-alanine) forms α-helical polypeptides at later stages, but strong ß-sheets of the L-alanine oligomers, which complicate NCA polymerization leading to broad and bimodal molecular weight distributions.[16] To mitigate this secondary structure-driven phenomenon, racemic alanine NCA mixtures were employed resulting in the successful synthesis of polyalanine with elevated molecular weights and narrow molecular weight distribution.[14]

In contrast to *per se* helix-forming amino acids, branching as well as the presence of a heteroatom (*O*/*S*) at the ß-carbon atom are both known to favour the formation of ß-sheets.[17] NCA polymerizations of isoleucine, valine, threonine, serine, and cysteine, thus, generally suffer from limited access to high molecular weights and narrow dispersities.[4,5,18] To overcome these limitations, again, racemic NCA mixtures have been employed for valine and isoleucine.[15,19–21] For polymerization of L-serine, L-threonine and L-cysteine NCAs, mostly, modifications were

introduced to the ß-heteroatom either weakening the ß-sheet structure or changing the preferred conformation to an α-helix supporting the chain growth.[20,22–25]

Among the 20 natural amino acids, cysteine takes a unique role due to its ability to stabilize proteins by (bio-) reversible disulfide bonds.[26,27] To transfer this feature to synthetic polymers for an application as "smart" or stimuli-responsive material, we previously reported on the *S*-alkylsulfonyl protecting group, which allows for nucleophilic amine-initiated polymerization of *S*-(ethylsulfonyl)-L-cysteine NCA and consecutive formation of asymmetric disulfide bonds with thiols (soft nucleophiles).[28,29] Moreover, block copolymers of poly(sarcosine)-*block*-poly(*S*-ethylsulfonyl-L-cysteine), so-called polypept(o)ides,[30,31] could be successfully employed to prepare disulfide cross-linked polymeric micelles and nanohydrogels.[32] Nevertheless, the polymerization of *S*-(ethylsufonly)-L-cysteine NCA was shown to be hampered by the formation of anti-parallel ß-sheets reducing the polymerization rate constants, lowering monomer conversion rates, and limiting accessible molecular weights.[29]

The aim of this work is now to investigate the nucleophilic ring-opening polymerization of racemic *S*-(ethylsulfonyl)-DL-cysteine *N*-carboxyanhydrides (NCA), to analyze the secondary structure of resulting homopolymers, and to incorporate these reactive amino acids into triblock copolymers.

Results and Discussion

To obtain *S*-(ethylsulfonyl)-DL-cysteine NCA (DL-Cys(SO$_2$Et) NCA), the corresponding amino acid, *S*-(ethylsulfonyl)-DL-cysteine, was synthesized from racemic cysteine hydrochloride by *S*-nitrosation (umpolung reaction) and *in situ* reaction with sodium ethylsulfinate, similar to previous reports on the L-enantiomer compound.[28,29] The NCA was prepared according to the Fuchs-Farthing method using diphosgene in tetrahydrofuran (THF) (Figure 1a).[33–35] Melting points of DL-Cys(SO$_2$Et) NCA (mp = 86 - 89°C) were significantly lower, compared to the L-enantiomer (mp = 113 - 115°C) compound.[36] From crystallization attempts of the racemic mixture, only crystals of the D-enantiomer could be isolated and analysed by X-ray crystallography (Figure S1 - S3), revealing NCA monomers arranged as an endless chain along the b-axis, mediated by N-H···O hydrogen bonds, which corresponds well with the previously published crystal structure of L-Cys(SO$_2$Et) NCA.[36]

ROP of DL-Cys(SO$_2$Et) NCA was performed at -10 °C in dry and purified N,N-dimethyl formamide (DMF) using neopentylamine as initiator (Figure 1a). These conditions have been reported optimal to ensure controlled living polymerization of L-Cys(SO$_2$Et) NCA, since the S-ethylsulfonyl protecting group remains intact during nucleophilic amine-initiated NCA polymerization, but can be used for consecutive disulfide bond formation with soft nucleophile thiols.[29,37]

For the synthesis of poly(S-ethylsulfonyl-DL-cysteine) (p(DL)Cys(SO$_2$Et)), racemic Cys(SO$_2$Et) NCA could be polymerized with high conversion rates of 89 - 100%, according to IR spectroscopy. As summarized in Table 1, the intended chain lengths are in well agreement with the results obtained from end-group analysis by NMR, and polypeptides with chain lengths from $X_n = 8$ to 102 with molecular weights up to 20.0 kDa could be successfully synthesized. Analysis by gel permeation chromatography (GPC) in hexafluoroisopropanol (HFIP) shows symmetric and monomodal molecular weight distributions for all polymers with well-defined dispersity ($Đ = 1.19$ to 1.33), relative to poly(methyl methacrylate) (PMMA) standards. A clear shift in the elution volume maximum can be detected by GPC, indicating controlled polymerization and valid chain lengths (Figure 1b and S4). The integrity of the polymer backbone as well as the reactive S-ethylsulfonyl protecting group was confirmed by the presence of only a single polymeric species in diffusion ordered spectroscopy (DOSY) NMR (Figure 1c) with all polymer signals being aligned. Furthermore, CD spectroscopy in HFIP verified the racemic nature of the isolated p(DL)Cys(SO$_2$Et) homopolymers, since no prevalent signal could be detected (Figure 1d).

In comparison to the results published on p(L)Cys(SO$_2$Et), indeed, longer chain lengths and higher conversion rates could be obtained from the racemic NCA.[29] For p(L)Cys(SO$_2$Et), the maximum chain length reported was $X_n = 43$, although, due to the formation of aggregates induced by strong anti-parallel β-sheets, multimodal molecular weight distributions were detected in HFIP GPC. While for p(L)Cys(SO$_2$Et) homopolymers with up to 20 repeating units narrow and symmetric molecular weight distributions were reported, chain lengths above $X_n = 20$ resulted in asymmetric distributions, which turned multimodal above $X_n = 30$.[29] In case of p(DL)Cys(SO$_2$Et), for chain lengths up to $X_n = 102$, symmetric molecular weight distributions and no aggregates were detected by HFIP GPC, thus facilitating polymer analysis and interpretation of the results (see Table 1 and Figure 1). For the synthesis of even higher molecular weights (M/I = 150), however, increased tailing was observed, as discussed further below.
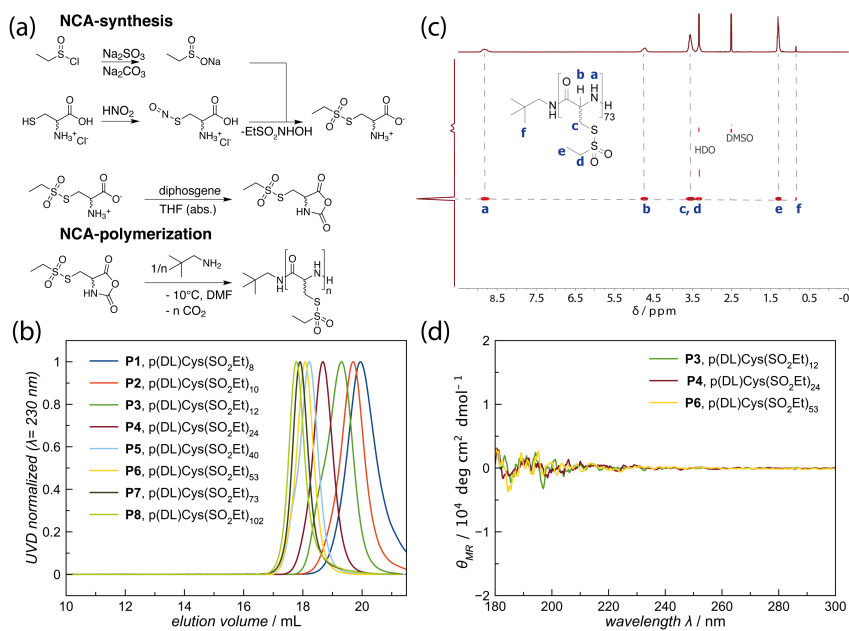
Figure 1. (**a**) Synthesis and ring-opening polymerization of *S*-ethylsulfonyl-DL-cysteine *N*-carboxyanhydride. (**b**) Analytical gel permeation chromatography in hexafluoro-isopropanol (HFIP GPC) of P1 to P8 indicates symmetric molecular weight distributions and a clear shift towards higher molecular weights with increasing monomer to initiator ratio. (**c**) DOSY NMR for p(DL)Cys(SO$_2$Et)$_{73}$ reveals the presence of only a single polymer species. (**d**) CD spectroscopy in HFIP does not give a prevalent signal irrespective of the polymer chain length, as expected for racemic compounds.

Table 1. Polymerization of *S*-(ethylsulfonyl)-DL-cysteine NCA.

No.	M/I	Conversion[a] / %	X_n[b]	M_n[b] / kDa	M_n[c] / kDa	Đ[c]
P1	4	100	8	1.65	2.92	1.31
P2	8	100	10	2.04	4.16	1.22
P3	15	100	12	2.43	6.20	1.21
P4	30	100	24	4.77	10.1	1.20
P5	40	100	40	7.90	18.0	1.24
P6	50	100	53	10.4	20.9	1.19
P7	75	89	73	14.3	23.8	1.27
P8	100	91	102	20.0	25.9	1.33

[a] based on IR spectroscopy, [b] end-group analysis by ^{1}H NMR, [c] HFIP GPC relative to PMMA standards.

To reveal the secondary structure of p(DL)Cys(SO$_2$Et), the racemic polypeptides were analysed by IR spectroscopy in solid state. As shown in Figure 2a, vibrational amide bands were detected at 1637 cm^{-1} (amide I), 1509 cm^{-1} (amide II), and 703 cm^{-1} (amide V), indicating β-sheet secondary structure, while the weak shoulder at 1702 cm^{-1} suggests their anti-parallel orientation.[38,39] No chain length dependencies were detected for the general position of the amide bands, whereas the shoulder at 1702 cm^{-1} becomes more evident with increasing chain lengths. For comparison, p(L)Cys(SO$_2$Et), which is known to adopt an anti-parallel β-sheet structure, shows similar wave numbers for the vibrational amide bands, but a distinct peak at 1702 cm^{-1} for p(L)Cys(SO$_2$Et)$_{13}$ (Figure 2a and S7, dashed green line).[29] In conclusion, p(DL)Cys(SO$_2$Et) seems to adopt β-sheet secondary structure with weakly pronounced anti-parallel orientation.[40,41] In contrast, poly(S-ethylsulfonyl-L-homocysteine), bearing the same reactive protecting group, displays wavelength-dependent helix-formation (1652 cm^{-1}) in solid state, and a fraction of aggregated protein structure (1625 cm^{-1}) disappears with increasing chain lengths (see Figure S7).

Since IR spectroscopy does not allow for reliable analysis of the polypeptide tacticity, ^{1}H NMR spectra of racemic p(DL)Cys(SO$_2$Et) and enantiopure p(L)Cys(SO$_2$Et) in dimethyl sulfoxide were employed for comparison.[42,43] In absence of racemisation, enantiopure NCAs are known to form isotactic polypeptides, whereas the polymerization of racemic NCA mixtures can be considered a copolymerization, leading to an overall atactic polymer with only short isotactic sequences, unless stereoselective or guiding templates are involved.[42,44,45] In our case, polymerization is conducted in solution without any additional driving force. As such, the signals of the racemic homopolymers (Figure 2b, upper spectrum) appear to be much broader than those of purely isotactic p(L)Cys(SO$_2$Et) (Figure 2b, lower spectrum), which suggests the rather atactic nature of the prepared p(DL)Cys(SO$_2$Et) homopolymers. For a detailed understanding, however, further studies are required.

To gain deeper insight into the polymerization of DL-Cys(SO$_2$Et) NCA, the kinetic behaviour was investigated *via* IR spectroscopy. The carbonyl stretching bands at 1858 and 1788 cm^{-1} were monitored over the course of 5 days and the integrals analysed, which correspond to the monomer concentration.

The majority of NCAs investigated to date (e.g. γ-(benzyl)-L-glutamic acid NCA, N-ε-(carbobenzoxy)-L-lysine NCA) are known to adopt an α-helical conformation, after a short initiation period, resulting in pseudo first-order kinetics in polar

solvents (e.g. DMF).[1,5,20] In contrast, cysteine NCA-derivatives are known to form ß-sheets upon polymerization.[20] Exemptions were only reported when large polar (e.g. oligoethylene glycol) or bulky side-groups (e.g. menthyl) have been introduced *via* thioether bonds.[25,46] *Vice versa*, during the polymerization of *S*-(methyl)-L-cysteine NCA, Kawai *et al.* observed secondary structure-driven crystallization hampering polymerization progress.
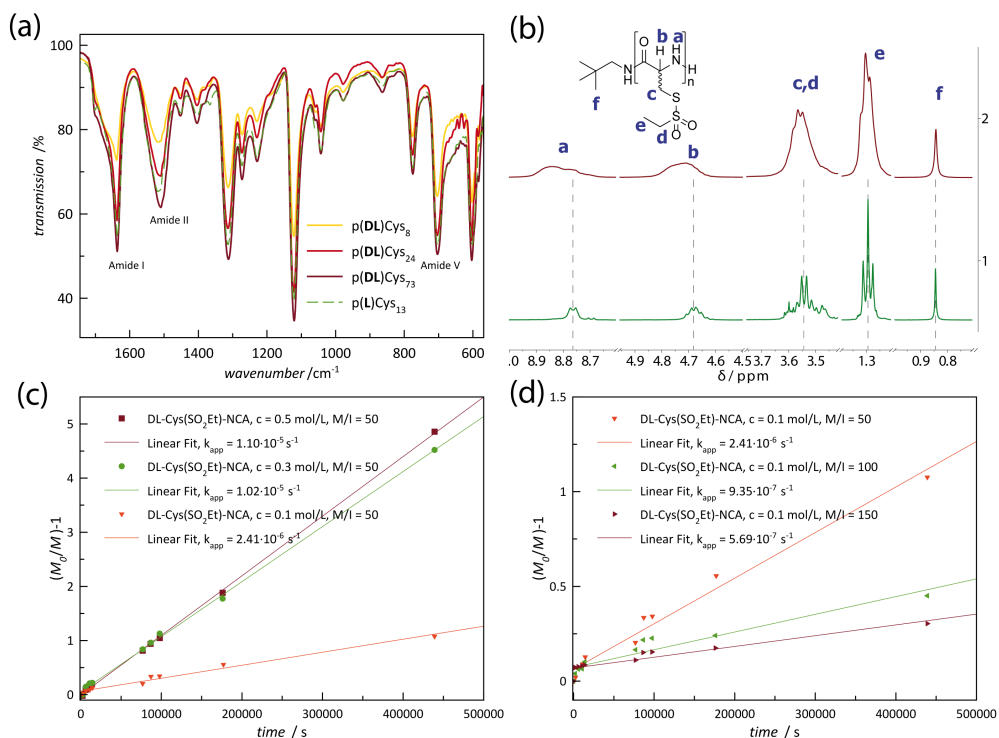

Figure 2. Secondary structure analysis and kinetic investigations. (**a**) Infrared spectroscopy (solid state) of racemic and enantiopure poly(*S*-ethylsulfonyl cysteine) with chain lengths of 8 to 73. (**b**) NMR spectroscopy of p(DL)Cys(SO₂Et)₂₂ (upper) and p(L)Cys(SO₂Et)₁₇ (lower) in DMSO-*d₆*. (**c**) Kinetic plot of p(DL)Cys(SO₂Et), M/I = 50 at varying monomer concentrations. (**d**) Kinetic plot of p(DL)Cys(SO₂Et), c_{NCA} = 0.1 mol·L⁻¹ with varying monomer to initiator ratios.

Instead of first-order kinetics, the polymerization behaviour could be described by the Avrami-equation.[12] As suggested by Iguchi, the Avrami equation, originally developed for crystallization kinetics, can be applied to describe a polymerization system which starts as a homogenous mixture but turns heterogenous throughout

polymerization.[47] No transfer or chemical termination reactions occur, but the association of oligomers leads to soluble (nano-) crystallites ultimately leading to physical termination, as the growing chain-end loses its mobility. Further growth is only possible at the surface.[13,47] The adapted Avrami equation is given by[29,47]

$$\frac{\delta(x)}{\delta(t)} = k \, [I][M_0] \left(1 - \frac{x}{[M_0]}\right)^2 \tag{1}$$

with $[M_0]$ is the initial monomer concentration; $[I]$ is the initiator concentration; $x = [M_0] - [M_t]$ is the consumed monomer at time t; and k is the rate constant, and can also be written as:[29]

$$\frac{\delta(x)}{\delta(t)} = k \, [I] \frac{[M_t]^2}{[M_0]} \tag{2}$$

It can thus be derived as

$$\frac{[M_0]}{[M_t]} = k \, [I] \, t + 1 \tag{3}$$

By plotting $\frac{[M_0]}{[M_t]} - 1$ versus the reaction time (t), the apparent rate constant of the polymerization ($k_{app} = k_p \cdot [I]$) as well as the polymerization rate (k_p) can be calculated. As shown in Figure 2c and Figure 2d, the experimental values obtained from IR spectroscopy follow the derived linear dependency. At constant monomer to initiator ratio, apparent rate constants increase with increasing monomer concentration, and decrease with increasing monomer to initiator ratio, when the monomer concentration is kept constant. In a similar manner, the polymerization of L-Cys(SO$_2$Et) NCA was reported to follow the Avrami-model, and both polymerizations seem to be affected by the formation of insoluble crystallites which govern the general polymerization behaviour qualitatively.[29] In contrast, S-ethylsulfonyl-L-homocysteine (L-Hcy(SO$_2$Et)) NCA showed fast pseudo first-order kinetics typically observed for α-helical polymerization.[48] When comparing the (apparent) rate constants, as summarized in Table 2, racemic DL-Cys(SO$_2$Et) NCA polymerizes slightly faster than L-Cys(SO$_2$Et) NCA (40% on average). This observation also reflects on the weaker secondary structure indicated by IR spectroscopy (Figure 2a), the increased solubility (HFIP GPC, Figure 1b), the rather atactic polymer structure, as detected by NMR spectroscopy (Figure 2b), as well as the obtained higher molecular weights.

Table 2. Polymerization kinetics. Apparent rate constants (k_{app}) and rate constants (k_p) for the ring-opening polymerization of *S*-(ethylsulfonyl)-protected NCA monomers.

NCA monomer	c_{NCA} [mol·L^{-1}]	k_{app} [s^{-1}]	k_p [L·mol^{-1} s^{-1}]
	0.1	$2.41 \cdot 10^{-6}$	$1.21 \cdot 10^{-3}$
DL-Cys(SO$_2$Et)	0.3	$1.02 \cdot 10^{-5}$	$1.70 \cdot 10^{-3}$
	0.5	$1.10 \cdot 10^{-5}$	$1.10 \cdot 10^{-3}$
	0.17	$3.43 \cdot 10^{-6}$	$1.01 \cdot 10^{-3}$
L-Cys(SO$_2$Et)	0.43	$8.09 \cdot 10^{-6}$	$9.41 \cdot 10^{-4}$
	0.59	$1.13 \cdot 10^{-5}$	$9.58 \cdot 10^{-4}$
	0.1	$1.44 \cdot 10^{-5}$	$7.20 \cdot 10^{-3}$
L-Hcy(SO$_2$Et)	0.3	$4.33 \cdot 10^{-5}$	$7.22 \cdot 10^{-3}$
	0.5	$5.29 \cdot 10^{-5}$	$5.29 \cdot 10^{-3}$

[a] values taken/calculated from Schäfer *et al*.[29]; [b] values taken/calculated from Muhl *et al*.[48]

Nevertheless, for DL-Cys(SO$_2$Et) NCA, the discrepancy among the reaction performed at a monomer concentration of 0.3 mol·L^{-1} versus 0.5 mol·L^{-1} is not significant, and similar conversions were detected for each time point. In agreement with these findings, certain limitations were detected for the polymerization of DL-Cys(SO$_2$Et) NCA. As shown in Figure S5a, the monomer concentration has a major impact on the reaction. Polymerizations at high NCA concentration (β_{NCA} = 100 g·L^{-1}, c_{NCA} = 0.42 mol·L^{-1}) lead to gelation after 50% conversion, resulting in low molecular weight polymers and bimodal GPC elugrams (see also Figure S6). On the other hand, low NCA concentrations (β_{NCA} = 30 g·L^{-1}, c_{NCA} = 0.13 mol·L^{-1}) result in slow polymerization progress and only low molecular weight polymers, even though high NCA conversions were achieved after 6 weeks at -10 °C. Medium NCA concentrations (β_{NCA} = 60 g·L^{-1}, c_{NCA} = 0.25 mol·L^{-1}) finally granted polymer synthesis up to chain lengths of X_n = 102 with well-defined polydispersity index (PDI). However, increased tailing and no significant shift in the maximum elution volume was detected for M/I ratio of 150 (Figure S5b), even though polymerization was carried out at similar conditions in purified and dry DMF (<50 ppm water). Interestingly, for p(L)Cys(SO$_2$Et), gelation was not observed until monomer concentrations above 0.8 mol·L^{-1}.[29]

Since we generally found high conversion rates for the polymerization of DL-Cys(SO$_2$Et) NCA, we aimed to exploit the racemic NCA for the synthesis of block co-polypept(o)ides. As illustrated in Figure 3a, the triblock copolymer,

p(L)Glu(OBn)-*b*-p(DL)Cys(SO$_2$Et)-*b*-pSar, with poly(*S*-ethylsulfonyl-DL-cysteine) as the middle block, was prepared by sequential NCA addition, after full conversion of the predecessor monomer was ensured by IR spectroscopy. Of note, due to incomplete conversion, the displayed sequence would require an additional intermediate work-up step if the enantiopure (L)Cys(SO$_2$Et) NCA was used. The results of the triblock copolymer synthesis are given in Figure 3 and summarized in Table S1. As shown, the calculated block lengths are in well agreement with the results obtained from end-group analysis in NMR (Figure 3b). More importantly, symmetric and monomodal molecular weight distributions could be observed for each reaction step by HFIP GPC. The clear shift in the elution volume maximum without significant tailing underlines the controlled living nature of the polymerization. In addition, the final polymers displayed molecular weights of 19400 g·mol^{-1} (diblock, p(L)Glu(OBn)-*b*-p(DL)Cys(SO$_2$Et)) and 33200 g·mol^{-1} (triblock, p(L)Glu(OBn)-*b*-p(DL)Cys(SO$_2$Et)-*b*-pSar,) as well as well-defined polymer dispersities of 1.23 and 1.43, relative to PMMA standards (see Figure 3c and Table S1).

Since the individual GPC curves are not baseline-separated, due to the chosen block length values, which are ideal with respect to polypeptide solubility, we investigated the absence of homopolymers by DOSY NMR spectroscopy. As a result of the reduced size of homopolymers, compared to consecutive diblock and triblock copolymers, monomodal peaks at a distinct diffusion index would broaden, become multimodal or, in the case of homopolymers coexisting with triblock copolymers, even two distinct species appear. As displayed in Figure 3d and S18, we observed only one diffusing species with narrow diffusion index distribution for diblock as well as triblock copolymers. Therefore, DOSY NMR experiments confirm successful block copolymer synthesis by controlled living ROP, which specifies the applicability of the racemic DL-Cys(SO$_2$Et) NCA for the synthesis of thiol-reactive block copolymers.
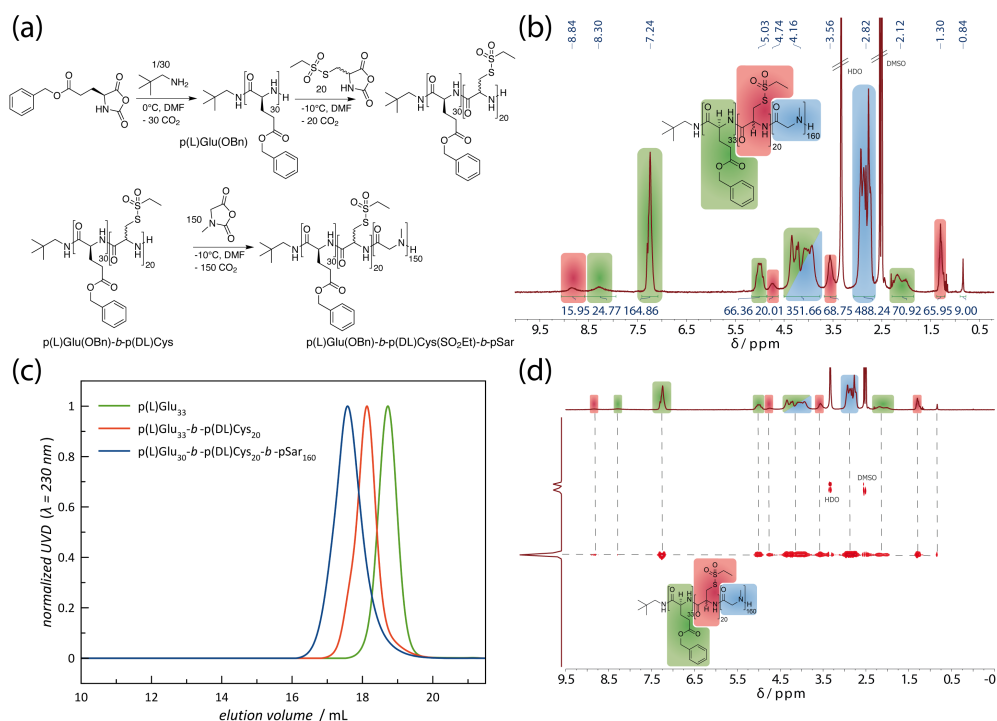
Figure 3. Triblock copolymer synthesis. (**a**) Synthesis of p(L)Glu(OBn)$_{30}$-*b*-p(DL)Cys(SO$_2$Et)$_{20}$-*b*-pSar$_{150}$ *via* sequential NCA polymerization. (**b**) End-group analysis by ^{1}H NMR spectroscopy. (**c**) Analytical HFIP GPC of the respective block sequences. For better visualization, p(L)Glu and p(DL)Cys were used as abbreviations for p(L)Glu(OBn) and p(DL)Cys(SO$_2$Et). (**d**) DOSY NMR indicates the presence of only a one diffusing polymer species.

Conclusion

We found that racemic DL-Cys(SO$_2$Et) NCAs can be successfully prepared and polymerized yielding well-defined homopolymers with symmetric molecular weight distributions for molecular weights up to 20.0 kDa, corresponding to an average degree of polymerization of 102 (determined by end-group analysis). To the best of our knowledge, for polypeptides forming β-sheets, this is the first comprehensive study on the use of racemic NCAs to improve their polymerization. The polymerization of DL-Cys(SO$_2$Et) NCA follows the Avrami-model for heterogenous polymerization, even though the formation of anti-parallel β-sheets was found to seem less pronounced than for purely isotactic p(L)Cys(SO$_2$Et),

resulting in slightly faster polymerization rates and full monomer conversion. As a consequence, the synthesis of triblock copolymers by sequential copolymerization can be achieved with excellent control over individual block lengths. Future research will thus address the question of how a reduced tendency for secondary structure formation affects the solution self-assembly of p(DL)Cys(SO₂Et)-containing block copolymers and the properties of nanoparticles thereof.

Experimental Section

Materials and Methods: Unless stated otherwise, reagents and solvents were purchased from Sigma Aldrich and used as received. THF was dried over Na and freshly distilled prior to use. DMF was bought from Acros (99.8%, extra dry over molecular sieve) and purified by repetitive freeze-pump thaw cycles to remove dimethylamine prior to use (water content < 50 ppm). Neopentylamine was purified by distillation over calcium hydride and stored over activated molecular sieves before further use. HFIP was purchased from Fluorochem. Deuterated solvents were obtained from Deutero GmbH and were used as received. ^{1}H NMR spectra were recorded on a Bruker Avance II 400 at room temperature at a frequency of 400 MHz. DOSY spectra were recorded on a Bruker Avance III HD 400 (400 MHz). Calibration of the spectra was achieved using the solvent signals. NMR spectra were analyzed with MestReNova version 12.0.4 from Mestrelab Research S.L. Degrees of polymerization (X_n) by ^{1}H NMR were calculated comparing the integral of the initiator peak and the integrals of the α-protons. Attenuated total reflectance Fourier transform infrared (ATR-FT-IR) spectroscopy was performed on a FT/IR-4100 (JASCO Corporation) with an ATR sampling accessory (MIRacle, Pike Technologies). IR spectra were analyzed using Spectra Manager 2.0 (JASCO Corporation). NCA polymerization was monitored by FT-IR spectroscopy. Polymerization was judged to be completed when NCA associated carbonyl peaks at 1858 and 1788 cm^{-1} had vanished. Analytical GPC was performed on a Jasco GPC setup at a flow rate of 0.8 ml·min^{-1} and a temperature of 40 °C. The eluent was HFIP equipped with 3 g·L^{-1} potassium trifluoroacetate. The column material was modified silica gel (PFG columns, particle size: 7 μm, porosity: 100 Å and 4000 Å), purchased from PSS Polymer Standards Service GmbH. For polymer detection, a UV detector (Jasco UV-2075+) at a wavelength of $\lambda = 230$ nm was employed. Molecular weights were determined by using a calibration with PMMA (PSS Polymer Standards Services GmbH) with

toluene as internal standard. The elution diagram was evaluated with PSS WinGPC (PSS Polymer Standard Service GmbH). Circular dichroism (CD) spectroscopy was performed on a Jasco J-815 spectrometer at room temperature and Spectra Manager 2.0 (Jasco) was used to analyze the spectra. A cell with a path length of 1 mm was used. Spectra were recorded at a concentration of 0.1 g·L^{-1} polymer in HFIP. Θ_{MR} was calculated using the equation with $M_{repeating\ unit}$ = 195.26 g·mol^{-1}, c_M = 0.1 g·L^{-1} and l = 0.1 cm for (Cys(SO$_2$Et)).

$$\theta_{MR} = \frac{\theta \,\cdot\, M_{repeating\ unit}}{10 \,\cdot\, l \,\cdot\, c_M} \ [\text{deg}\cdot \text{cm}^2 \cdot \text{dmol}^{-1}]$$

Synthesis of Sodium Ethylsulfinate: The synthesis of sodium ethylsulfinate was adapted from literature.[28]

A solution of sodium sulfite (142.6 g, 1.38 mol, 3.5 eq.) in water (275 mL) was heated to 80 °C. Ethanesulfonyl chloride (37.6 mL, 50.84 g, 0.395 mol, 1.0 eq.) and sodium carbonate (84.09 g, 0.793 mol) were added simultaneously while significant quantities of CO$_2$ evolved. The reaction mixture was stirred for one hour at 80 °C. Next, the solvent was removed *in vacuo* at 40 °C. The resulting solid was suspended in methanol (approx. 300 mL) and filtered to remove sodium carbonate and side products. Evaporation of methanol yielded sodium ethylsulfinate (45.0 g, 0.388 mol, 98%) as a colorless solid.

^{1}H NMR (400 MHz, D$_2$O + TFA-d_1), δ [ppm] = 2.32 (q, ^3J = 7.6 Hz, 2H, -*CH$_2$*-), 1.06 (t, ^3J = 7.6 Hz, 3H, -*CH$_3$*).

Synthesis of *S*-(Ethylsulfonyl)-DL-Cysteine: An ice-cold solution of sodium nitrite (9.90 g, 144 mmol, 1.0 eq.) in degassed water (125 mL) was slowly added to a stirred solution of DL-cysteine hydrochloride (22.6 g, 144 mmol, 1.0 eq.) in previously degassed 2N HCl (150 mL) at a temperature of 0 °C. After 1 h, sodium ethylsulfinate (44.5 g, 388 mmol, 2.7 eq.) was added to the deep red solution in one portion. After 5 minutes, a colorless solid precipitated. The suspension was stirred for additional 5 h at 0 °C and was stirred at room temperature overnight. The precipitate was collected and washed with methanol to remove residual sulfinate. The product was dried *in vacuo* yielding *S*-(ethylsulfonyl)-DL-cysteine (13.5 g, 63.3 mmol, 44%) as a colorless powder.

^{1}H NMR (400 MHz, D$_2$O + TFA-d_1), δ [ppm] = 4.44 (dd, ^3J = 6.7 Hz, ^3J = 4.5 Hz, 1H, α-*CH*), 3.72 (dd, ^2J = 15.6 Hz, ^3J = 4.5 Hz, 1H, -*CH$_2$*-CH-), 3.58 (dd, ^2J = 15.6

Hz, ^3J = 6.7 Hz, 1H, -CH_2-CH-), 3.50 (dq, ^3J = 7.3 Hz, ^3J = 1.66 Hz, 2H, -CH_2-CH$_3$), 1.39 (t, ^3J = 7.3 Hz, 3H, -CH_3).

Synthesis of *S*-(Ethylsulfonyl)-DL-Cysteine *N*-Carboxyanhydride: *S*-(Ethylsulfonyl)-DL-cysteine (7.00 g, 32.82 mmol) was dried by azeotropic distillation with toluene. Next, the amino acid was suspended in absolute THF (100 mL) and diphosgene (3.60 mL, 5.84 g, 29.52 mmol) was added slowly. The suspension was stirred at room temperature until a clear solution was obtained (approx. 3 h). To remove excess diphosgene, a stream of dry nitrogen was led through the reaction mixture into gas washing bottles, equipped with an aqueous NaOH solution, for 2 h. The remaining solvent was removed *in vacuo* and the residue was dissolved in dry dioxane. Any insoluble compounds were removed by filtration avoiding contact with air, and the NCA solution was slowly precipitated into a mixture of absolute diethyl ether/*n*-hexane (1:2). The precipitation of the product was repeated two more times yielding *S*-(ethylsulfonyl)-DL-cysteine NCA (6.43 g, 26.87 mmol, 82%) as a colorless powder. Absence of chloride impurities was verified by silver nitrate chloride test. mp = 88.5 °C at a heating rate of 7 °C/min, 86.1 °C at 5 °C/min under decomposition.

^{1}H NMR (400 MHz, DMSO-d_6), δ [ppm] = 9.34 (bs, 1H, NH), 4.85 (ddd, ^3J = 5.7 Hz, ^3J = 5.2 Hz, ^3J = 1.3 Hz, 1H, α-CH), 3.62 (m, 4H, -CH_2-CH- & -CH_2-CH$_3$), 1.29 (t, ^3J = 7.2 Hz, 3H, -CH_3).

For crystallization, dry *n*-hexane was added very carefully on top of an NCA solution in dry ethyl acetate and kept at -20 °C until the formation of colorless NCA crystals was completed.

Synthesis of Poly(*S*-Ethylsulfonyl-DL-Cysteine): DL-Cys(SO$_2$Et) NCA (54.8 mg, 229 µmol, 75 eq.) was transferred into a dried Schlenk-flask, dissolved in 0.78 mL of anhydrous DMF (freshly purified by freeze-thaw cycles) and cooled to -10 °C. Neopentylamine initiator (0.266 mg, 3.05 µmol, 1.0 eq.) was added as a stock solution in DMF (133 µL, β_{NPA} = 2.0 g·L^{-1}) yielding the reaction mixture with a final NCA concentration of 60 g·L^{-1}. A steady flow of dry nitrogen was sustained during the polymerization. The progress of the polymerization was monitored *via* FT-IR spectroscopy and judged to be completed when the carbonyl stretching bands of the NCA at 1858 and 1788 cm^{-1} had vanished. Samples were taken using a nitrogen flushed syringe trough a septum. Upon completed monomer conversion, the polymer was precipitated in a mixture of cold diethyl ether and THF (1:1, v/v). The suspension was centrifuged (4500 rpm, 15 min, 4°C) and

decanted. This procedure was repeated twice concluding with pure diethyl ether. The product was dried *in vacuo* yielding poly(*S*-ethylsulfonyl-DL-cysteine) (45 mg, 100%) as a colorless to slightly yellow solid.

Polymerizations conducted at lower NCA concentrations (β_{NCA} = 30 g·L^{-1}) resulted in slow polymerization progress, whereas higher NCA concentrations (β_{NCA} = 100 g·L^{-1}) resulted in gelation, yielding low molecular weight polymers for both cases, and polymerization at (β_{NCA} = 60 g·L^{-1}) appears to be optimal.

^{1}H NMR (400 MHz, DMSO-d_6), δ [ppm] = 8.84 (b s, 1n H, *NH*), 4.71 (b s, 1n H, α-*H*), 3.57 (b s, 4n H, -*CH$_2$*-CH- & -*CH$_2$*-CH$_3$), 1.30 (b s, 3n H, -*CH$_3$*), 0.84 (b s, 9H, -(*CH$_3$*)$_3$).

Kinetic Investigations: Polymerizations were prepared as described above and analyzed over a period of 5 d. Samples were taken using a nitrogen flushed syringe trough a septum. The decreasing NCA carbonyl peaks at 1858 and 1788 cm^{-1} were monitored and the integrals were correlated with the NCA concentration for kinetic evaluations.[49]

Synthesis of p(L)Glu(OBn)$_n$-b-p(DL)Cys(SO$_2$Et)$_m$-b-pSar$_o$: Additional *N*-carboxyanhydride monomers, sarcosine NCA and *γ*-benzyl-L-glutamate NCA, were prepared according to previous publications.[31,36]

L-Glu(OBn) NCA (240 mg, 912 µmol, 30 eq.) was transferred into a pre-dried Schlenk-flask, dissolved in 2.0 mL of anhydrous DMF and cooled to 0 °C. Neopentylamine initiator (2.65 mg, 30.4 µmol, 1.0 eq.) was added as a stock solution in DMF (265 µL, β_{NPA} = 10.0 g·L^{-1}) and a steady flow of dry nitrogen was sustained during the polymerization. After 3 days, upon completed L-Glu(OBn) NCA conversion, as detected by FT-IR spectroscopy, the reaction mixture was cooled to -10 °C and DL-Cys(SO$_2$Et) NCA (145 mg, 608 µmol, 20 eq.) was added as a stock solution in anhydrous DMF (72.5 µL, β_{NCA} = 200 g·L^{-1}). Upon completed DL-Cys(SO$_2$Et) NCA conversion after additional 6 days, sarcosine NCA (525 mg, 4.56 mmol, 150 eq.) was added as a stock solution in DMF (1.75 mL, β_{NCA} = 300 g·L^{-1}) and the polymerization continued at -10 °C. The reaction was judged to be completed after polymerization for further 19 days, with a total duration of 28 days. Next, the polymer was precipitated into THF. The suspension was centrifuged (4500 rpm, 15 min, 4 °C) and decanted. This procedure was repeated twice concluding with pure diethyl ether. For further purification, the polymer was dialyzed against MilliQ water (MWCO 6-8 kDa) for one day and obtained as a colorless powder (385 mg, 58%) from lyophilization of the aqueous solution. For

polymer analytics, samples (each 150 µL) were taken by syringe through the septum, after completion of the respective blocks, and precipitated in THF and diethyl ether as described above.

^{1}H NMR p(L)Glu(OBn)$_n$ (400 MHz, DMSO-d_6), δ [ppm] = 8.30 (b s, 1n H, *NH*), 7.24 (b s, 5n H, Arom. *CH*), 5.03 (m, 2n H, O-*CH$_2$*), 3.92 (m, 1n H, α-*CH*), 2.29 - 1.85 (m, 4n H, *β-CH$_2$*- & *γ-CH$_2$*-), 0.84 (b s, 9H, -(*CH$_3$*)$_3$).

^{1}H NMR p(L)Glu(OBn)$_n$-*b*-p(DL)Cys(SO$_2$Et)$_m$ (400 MHz, DMSO-d_6), δ [ppm] = 8.84 (b s, 1m H, *NH*), 8.30 (b s, 1n H, *NH*), 7.24 (b s, 5n H, Arom. *CH*), 5.03 (m, 2n H, O-*CH$_2$*), 4.74 (b s, 1m H, α-*CH*), 3.92 (m, 1n H, α-*CH*), 3.57 (b s, 4m H, *β-CH$_2$* & -*CH$_2$*-CH$_3$), 2.29 - 1.85 (m, 4n H, *β-CH$_2$*- & *γ-CH$_2$*-), 1.30 (m, 3o H, -*CH$_3$*), 0.84 (b s, 9H, -(*CH$_3$*)$_3$).

^{1}H NMR p(L)Glu(OBn)$_n$-*b*-p(DL)Cys(SO$_2$Et)$_m$-*b*-pSar$_o$ (400 MHz, DMSO-d_6), δ [ppm] = 8.84 (b s, 1m H, *NH*), 8.30 (b s, 1n H, *NH*), 7.24 (b s, 5n H, Arom. *CH*), 5.03 (m, 2n H, O-*CH$_2$*), 4.74 (b s, 1m H, α-*CH*), 4.50 - 3 77 (m, 1n H+ 2p H, α-*CH* & *CH$_2$*), 3.57 (b s, 4m H, -*CH$_2$*-CH- & -*CH$_2$*-CH$_3$), 3.07 - 2.67 (m, 3o H, -*CH$_3$*), 2.29 - 1.85 (m, 4n H, *β-CH$_2$*- & *γ-CH$_2$*-), 1.30 (m, 3o H, -*CH$_3$*), 0.84 (b s, 9H, -(*CH$_3$*)$_3$).

Notes

CCDC 2002425 contains the supplementary crystallographic data for this paper. These data can be obtained free of charge from The Cambridge Crystallographic Data Centre via www.ccdc.cam.ac.uk/data_request/cif.

Acknowledgements

References

(1)   Kricheldorf, H. R. Polypeptides and 100 Years of Chemistry of α-Amino Acid N-Carboxyanhydrides. *Angew. Chemie - Int. Ed.* **2006**, *45* (35), 5752–5784.

(2)   Birke, A.; Ling, J.; Barz, M. Polysarcosine-Containing Copolymers: Synthesis, Characterization, Self-Assembly, and Applications. *Prog. Polym. Sci.* **2018**, *81*, 163–208.

(3)   Huang, J.; Heise, A. Stimuli Responsive Synthetic Polypeptides Derived from N-Carboxyanhydride (NCA) Polymerisation. *Chem. Soc. Rev.* **2013**, *42* (17), 7373–

7390.

(4) Bonduelle, C. Secondary Structures of Synthetic Polypeptide Polymers. *Polym. Chem.* **2018**, *9* (13), 1517–1529.

(5) Szwarc, M. The Kinetics and Mechanism of N-Carboxy-α-Amino-Acid Anhydride (NCA) Polymerisation to Poly-Amino Acids. In *Adv. Polym. Sci.*; 1965; Vol. 4, 1–65.

(6) Cheng, J.; Deming, T. J. Synthesis of Polypeptides by Ring-Opening Polymerization of α-Amino Acid N-Carboxyanhydrides. In *Peptide-Based Materials*; **2011**; Vol. 310, 1–26.

(7) Huesmann, D.; Birke, A.; Klinker, K.; Türk, S.; Räder, H. J.; Barz, M. Revisiting Secondary Structures in NCA Polymerization: Influences on the Analysis of Protected Polylysines. *Macromolecules* **2014**, *47* (3), 928–936.

(8) Aliferis, T.; Iatrou, H.; Hadjichristidis, N. Living Polypeptides. *Biomacromolecules* **2004**, *5* (5), 1653–1656.

(9) Lundberg, R. D.; Doty, P. Polypeptides. XVII. A Study of the Kinetics of the Primary Amine-Initiated Polymerization of N-Carboxy-Anhydrides with Special Reference to Configurational and Stereochemical Effects. *J. Am. Chem. Soc.* **1957**, *79* (15), 3961–3972.

(10) Baumgartner, R.; Fu, H.; Song, Z.; Lin, Y.; Cheng, J. Cooperative Polymerization of α-Helices Induced by Macromolecular Architecture. *Nat. Chem.* **2017**, *9* (7), 614–622.

(11) Chen, C.; Fu, H.; Baumgartner, R.; Song, Z.; Lin, Y.; Cheng, J. Proximity-Induced Cooperative Polymerization in "Hinged" Helical Polypeptides. *J. Am. Chem. Soc.* **2019**, *141* (22), 8680–8683.

(12) Kawai, T.; Komoto, T. Crystallization of Polypeptides during Polymerization. *J. Cryst. Growth* **1980**, *48* (2), 259–282.

(13) Komoto, T.; Oya, M.; Kawai, T. Crystallization of Polypeptides in the Course of Polymerization. *Macromol. Chem.* **1974**, *175* (1), 301–310.

(14) Kricheldorf, H. R.; von Lossow, C.; Schwarz, G. Primary Amine-Initiated Polymerizations of Alanine-NCA and Sarcosine-NCA. *Macromol. Chem. Phys.* **2004**, *205* (7), 918–924.

(15) Komoto, T.; Oya, M.; Kawai, T. Crystallization of Polypeptides in the Course of Polymerisation 5. *Macromol. Chem.* **1974**, *175*, 283–299.

(16) Kricheldorf, H. R.; Mutter, M.; Maser, F.; Müller, D.; Förster, H. Secondary Structure of Peptides. 4:13C-Nmr CP/MAS Investigation of Solid Oligo- and Poly(L-Alanines). *Biopolymers* **1983**, *22* (5), 1357–1372.

(17) Chou, P. Y.; Pasman, G. D. Conformational Parameters for Amino Acids in Helical, ß-Sheet, and Random Coil Regions Calculated from Proteins. *Biochemistry* **1974**, *13* (2), 211–222.

(18) Kricheldorf, H. R. Polypeptide Und 100 Jahre Chemie Der α-Aminosäure-N-Carboxyanhydride. *Angew. Chemie* **2006**, *118* (35), 5884–5917.

(19) Kricheldorf, H. R.; Von Lossow, C.; Schwarz, G. Cyclic Polypeptides by Solvent-Induced Polymerizations of α-Amino Acid n-Carboxyanhydrides. *Macromolecules* **2005**, *38* (13), 5513–5518.

(20) Deming, T. J. Synthesis of Side-Chain Modified Polypeptides. *Chem. Rev.* **2016**, *116*

(3), 786–808.

(21) Akaike, T.; Aogaki, Y.; Inoue, S. Stereochemistry of the D and L Copolymerization of Valine N-carboxyanhydride. *Biopolymers* **1975**, *14* (12), 2577–2583.

(22) Huesmann, D.; Klinker, K.; Barz, M. Orthogonally Reactive Amino Acids and End Groups in NCA Polymerization. *Polym. Chem.* **2016**, *8* (6), 957–971.

(23) Hwang, J.; Deming, T. J. Methylated Mono- and Di(Ethylene Glycol)-Functionalized ß-Sheet Forming Polypeptides. *Biomacromolecules* **2001**, *2* (1), 17–21.

(24) Hayakawa, T.; Matsuyama, M.; Inouye, K. Poly(S-Alkyl-l-Cysteines) Containing Long Aliphatic Side Chains. *Polymer (Guildf).* **1977**, *18* (8), 854–855.

(25) Hayakawa, T.; Kondo, Y.; Matsuyama, M. Syntheses and Conformational Studies of Poly(S-Menthyloxycarbonylmethyl l- and d-Cysteines). *Polymer (Guildf).* **1976**, *17* (11), 1009–1012.

(26) Berger, A.; Noguchi, J.; Katchalski, E. Poly-L-Cysteine. *J. Am. Chem. Soc.* **1956**, *78* (17), 4483–4488.

(27) Poole, L. B. The Basics of Thiols and Cysteines in Redox Biology and Chemistry. *Free Radic. Biol. Med.* **2015**, *80*, 148–157.

(28) Schäfer, O.; Huesmann, D.; Muhl, C.; Barz, M. Rethinking Cysteine Protective Groups: S -Alkylsulfonyl- l -Cysteines for Chemoselective Disulfide Formation. *Chem. - A Eur. J.* **2016**, *22* (50), 18085–18091.

(29) Schäfer, O.; Huesmann, D.; Barz, M. Poly(S -Ethylsulfonyl- l -Cysteines) for Chemoselective Disulfide Formation. *Macromolecules* **2016**, *49* (21), 8146–8153.

(30) Klinker, K.; Barz, M. Polypept(o)Ides: Hybrid Systems Based on Polypeptides and Polypeptoids. *Macromol. Rapid Commun.* **2015**, *36* (22), 1943–1957.

(31) Birke, A.; Huesmann, D.; Kelsch, A.; Weilbächer, M.; Xie, J.; Bros, M.; Bopp, T.; Becker, C.; Landfester, K.; Barz, M. Polypeptoid- Block -Polypeptide Copolymers: Synthesis, Characterization, and Application of Amphiphilic Block Copolypept(o)Ides in Drug Formulations and Miniemulsion Techniques. *Biomacromolecules* **2014**, *15* (2), 548–557.

(32) Klinker, K.; Schäfer, O.; Huesmann, D.; Bauer, T.; Capelôa, L.; Braun, L.; Stergiou, N.; Schinnerer, M.; Dirisala, A.; Miyata, K.; Osada, K.; Cabral, H.; Kataoka, K.; Barz, M. Secondary-Structure-Driven Self-Assembly of Reactive Polypept(o)Ides: Controlling Size, Shape, and Function of Core Cross-Linked Nanostructures. *Angew. Chemie Int. Ed.* **2017**, *56* (32), 9608–9613.

(33) Farthing, A. C.; Reynolds, R. J. W. Anhydro-N-Carboxy-DL-ß-Phenylalanine. *Nature* **1950**, *165* (4199), 647–647.

(34) Fuchs, F. Über N-Carbonsäure-Anhydride. *Chem. Ber.* **1922**, *55B*, 2943.

(35) Fetsch, C.; Grossmann, A.; Holz, L.; Nawroth, J. F.; Luxenhofer, R. Polypeptoids from N -Substituted Glycine N -Carboxyanhydrides: Hydrophilic, Hydrophobic, and Amphiphilic Polymers with Poisson Distribution. *Macromolecules* **2011**, *44* (17), 6746–6758.

(36) Schäfer, O.; Schollmeyer, D.; Birke, A.; Holm, R.; Johann, K.; Muhl, C.; Seidl, C.; Weber, B.; Barz, M. Investigation of α-Amino Acid N-Carboxyanhydrides by X-Ray Diffraction for Controlled Ring-Opening Polymerization. *Tetrahedron Lett.* **2019**, *60* (3), 272–275.

(37)   Barz, M.; Huesmann, D.; Schäfer, O.; Reuter, T.; Birke, A.; Heller, P. Thiol-Protected Amino Acid Derivatives and Uses Thereof, **2014**, EP2942348A1.

(38)   Pelton, J. T.; McLean, L. R. Spectroscopic Methods for Analysis of Protein Secondary Structure. *Anal. Biochem.* **2000**, *277* (2), 167–176.

(39)   Goormaghtigh, E.; Ruysschaert, J. M.; Raussens, V. Evaluation of the Information Content in Infrared Spectra for Protein Secondary Structure Determination. *Biophys. J.* **2006**, *90* (8), 2946–2957.

(40)   Pauling, L.; Corey, R. B. Two Rippled-Sheet Configurations of Polypeptide Chains, and a Note about the Pleated Sheets. *Proc. Natl. Acad. Sci.* **1953**, *39* (4), 253–256.

(41)   Nowick, J. S. Exploring β-Sheet Structure and Interactions with Chemical Model Systems. *Acc. Chem. Res.* **2008**, *41* (10), 1319–1330.

(42)   Kricheldorf, H. R.; Müller, D. Secondary Structure of Peptides. *Polym. Bull.* **1983**, *10* (11–12), 513–520.

(43)   Shapiro, Y. E. Analysis of Chain Microstructure by 1H and 13C NMR Spectroscopy. *Bull. Magn. Reson.* **1985**, *7*, 27–58.

(44)   Rubinstein, I.; Eliash, R.; Bolbach, G.; Weissbuch, I.; Lahav, M. Racemic β Sheets in Biochirogenesis. *Angew. Chemie* **2007**, *119* (20), 3784–3787.

(45)   Weissbuch, I.; Illos, R. A.; Bolbach, G.; Lahav, M. Racemic β-Sheets as Templates of Relevance to the Origin of Homochirality of Peptides: Lessons from Crystal Chemistry. *Acc. Chem. Res.* **2009**, *42* (8), 1128–1140.

(46)   Fu, X.; Shen, Y.; Fu, W.; Li, Z. Thermoresponsive Oligo(Ethylene Glycol) Functionalized Poly- l -Cysteine. *Macromolecules* **2013**, *46* (10), 3753–3760.

(47)   Iguchi, M. A Comment on the Kinetics in a Heterogeneous Polymerization System. *J. Polym. Sci. Part A-1 Polym. Chem.* **1970**, *8* (4), 1013–1021.

(48)   Muhl, C.; Schäfer, O.; Bauer, T.; Räder, H.-J.; Barz, M. Poly(S -Ethylsulfonyl- l -Homocysteine): An α-Helical Polypeptide for Chemoselective Disulfide Formation. *Macromolecules* **2018**, *51* (20), 8188–8196.

(49)   Idelson, M.; Blout, E. R. Polypeptides. XV. 1 Infrared Spectroscopy and the Kinetics of the Synthesis of Polypeptides: Primary Amine Initiated Reactions. *J. Am. Chem. Soc.* **1957**, *79* (15), 3948–3955.

Supporting Information

Results and Discussion

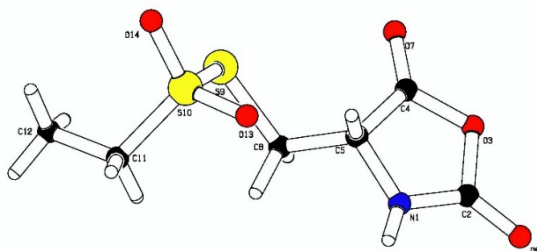### *X-Ray Crystal Structure Analysis*

Figure S1. XRD-Analysis of *S*-(ethylsulfonyl)-D-cysteine *N*-carboxyanhydride as crystallized from the racemic mixture.
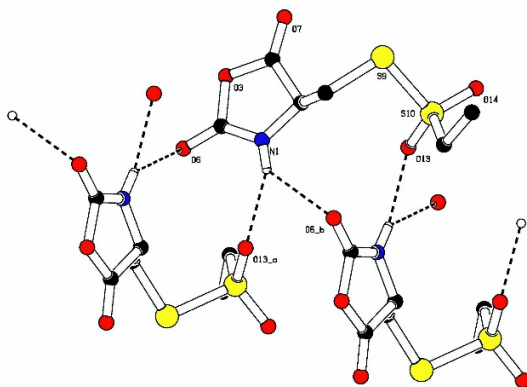

Figure S2. XRD-Analysis of *S*-(ethylsulfonyl)-D-cysteine *N*-carboxyanhydride. NCA monomers organize as linear chain *via* NH···O hydrogen bonds.
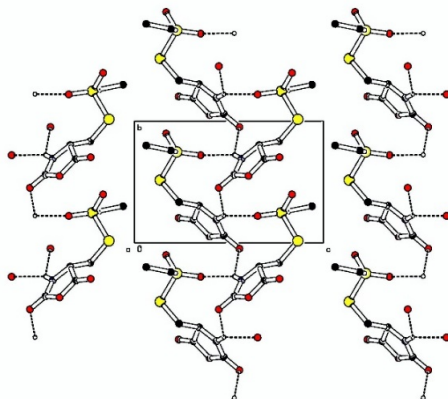
Figure S3. XRD-Analysis of *S*-(ethylsulfonyl)-D-cysteine *N*-carboxyanhydride. NCA monomers organize as linear chain along the b-axis *via* NH$\cdots$O hydrogen bonds.

Crystal Data for S-Ethylsulfonyl-D-Cysteine N-Carboxyanhydride

formula	$C_6H_9O_5NS_2$
molecular weight	239.27 g·mol^{-1}
absorption	$\mu = 0.55$ mm^{-1}
transmission	$T_{min} = 0.9064$, $T_{max} = 0.9675$
crystal size	0.06 x 0.08 x 0.25 mm^3 colourless block
space group	P 2$_1$ (monoclinic)

lattice parameters
(calculated from

$a =$ 5.9154(5)Å
$b =$ 7.2438(5)Å   ß = 102.667(8)°

3231 reflections with

$c =$ 11.5288(12)Å

2.3° < θ < 28.3°)

$V =$ 481.99(7)Å^3 z = 2   F(000) = 248

temperature	120K
density	$d_{xray} = 1.649$ g·cm^{-3}

Data Collection

diffractometer	STOE IPDS 2T
radiation	Mo-K$_\alpha$ Graphitmonochromator

Scan – type   ω scans

Scan – width   1°

scan range $2° \leq \theta < 28°$; $-7 \leq h \leq 7$ $-9 \leq k \leq 9$ $-14 \leq l \leq 15$

number of reflections:

measured   3464

unique   2286 (R_{int} = 0.0369)

observed   1810 ($|F|/\sigma(F) > 4.0$)

Data Correction, Structure Solution and Refinement

corrections   Lorentz and polarisation correction.

structure solution   Program: SIR-2004 (Direct methods)

refinement   Program: SHELXL-2018 (full matrix). 159 refined parameters, weighting scheme: $w=1/[\sigma^2(F_o^2) + (0.0514*P)^2]$

with $(Max(F_o^2,0)+2*F_c^2)/3$. H-atoms localized and refined with isotropic thermal parameters, non H- atoms refined anisotropically.

R-values   wR2 = 0.0949 (R1 = 0.0433 for observed reflections, 0.0634 for all reflections)

goodness of fit   S = 0.993

Flack parameter   x=-0.1(1)

maximum deviation of parameters   0.001 * e.s.d

maximum peak height in diff. Fourier synthesis   0.4, -0.29 eÅ^{-3}

Gel Permeation Chromatography
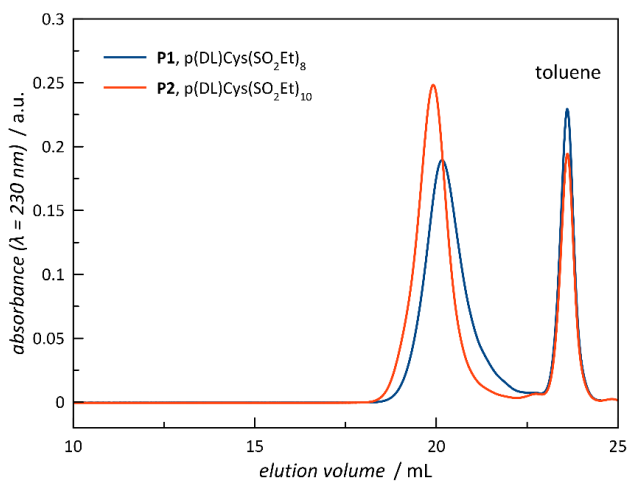
Figure S4. Analytical gel permeation chromatography in HFIP. UV-Detector signals (raw data) for poly(S-ethylsulfonyl-DL-cysteine) with short chain lengths (X_n = 8 to 10) show overlap with the internal standard (toluene).
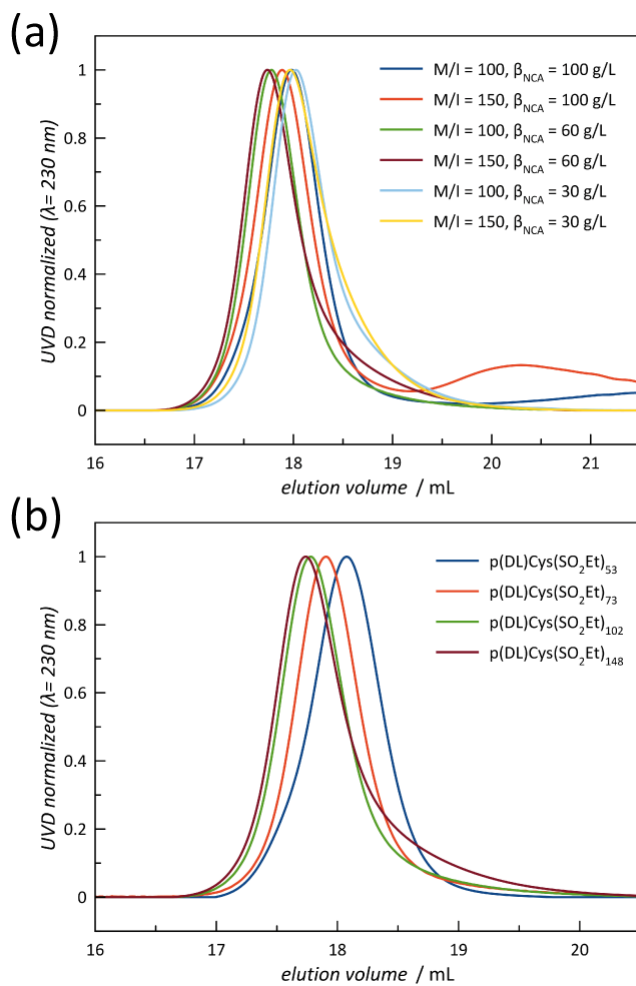
Figure S5. HFIP GPC indicates the limits of DL-Cys(SO₂Et) NCA polymerization. (**a**) Influence of the NCA concentration. (**b**) Influence of the monomer to initiator ratio.
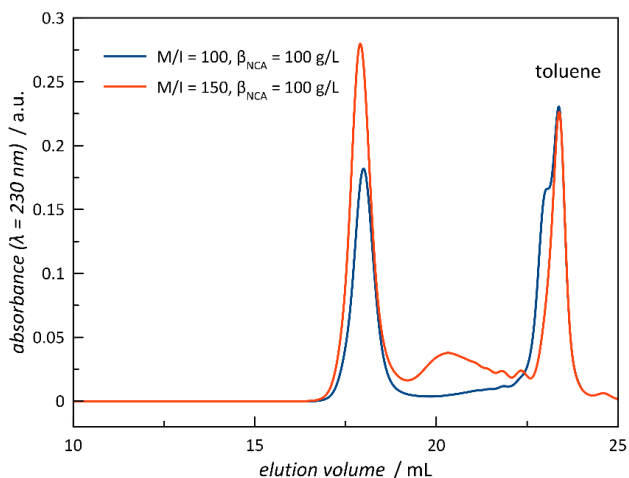
Figure S6. Analytical gel permeation chromatography in HFIP. UV-Detector signals (raw data) for the polymerization of S-ethylsulfonyl-DL-cysteine NCA at monomer to initiator ratios of 100 and 150 conducted at high NCA concentrations of $\beta_{NCA} = 100$ g $\cdot$L^{-1} result in broad molecular weight distributions and overlap with the signal of the internal standard (toluene).

Table S1. Analytical results of the triblock copolymer synthesis.

polymer	M/I (calc.)[a]	X_n(Glu)[b]	X_m(Cys)[b]	X_o(Sar)[b]	M_n[c] / kDa	Đ[c]
p(L)Glu(OBn)$_n$	30	33	-	-	10.1	1.10
p(L)Glu(OBn)$_n$-b-p(DL)Cys(SO$_2$Et)$_m$	20	33	20	-	19.4	1.23
p(L)Glu(OBn)$_n$-b-p(DL)Cys(SO$_2$Et)$_m$-b-pSar$_o$	150	33	20	160	33.2	1.43

[a] monomer to (macro-)initiator ratio calculated for the respective NCAs; [b] end-group analysis by ^{1}H NMR; [c] HFIP GPC relative to PMMA standards.

FT-IR-Spectroscopy
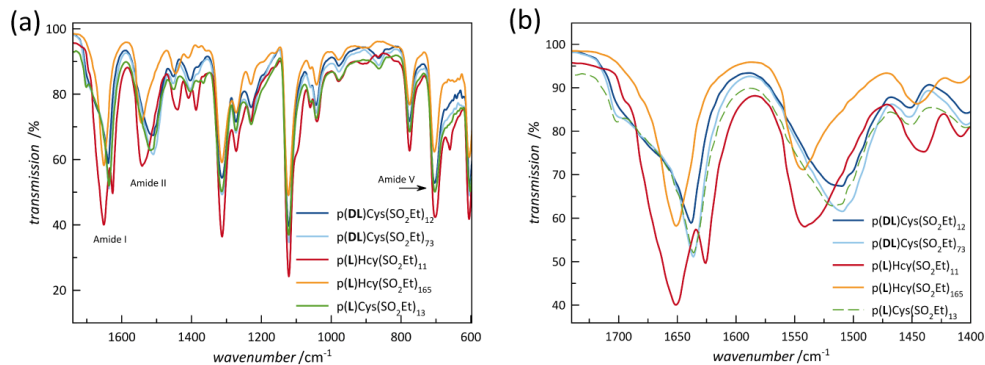
Figure S7. Infrared spectroscopy (solid state) of racemic and enantiopure poly(*S*-ethylsulfonyl-cysteine) and poly(*S*-ethylsulfonyl-L-homocysteine) (pHcy(SO₂Et)). pHcy(SO₂Et) shows wavelength-dependent helix formation.

NMR-Spectroscopy
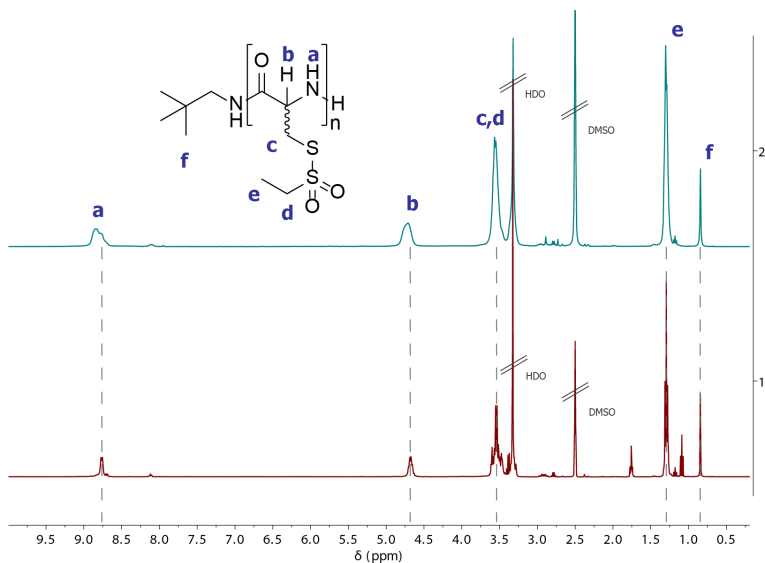
Figure S8. ^{1}H NMR of poly(*S*-ethylsulfonyl-DL-cysteine) (upper) shows broader signals compared to poly(*S*-ethylsulfonyl-L-cysteine) (lower) of similar chain length in DMSO-*d₆*, indicating atactic polymer structure.
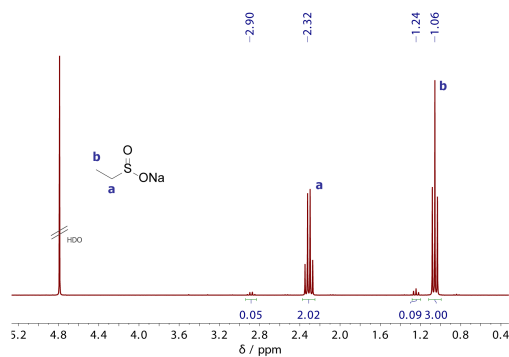
Figure S9. ^{1}H NMR spectrum of sodium ethylsulfinate in D_2O + TFA-d_1. Signals at 2.90 and 1.24 ppm indicate traces of oxidation product sodium ethanesulfonate (about 3%).
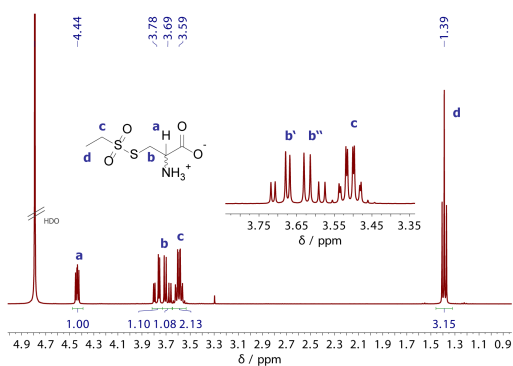
Figure S10. ^{1}H NMR spectrum of S-(ethylsulfonyl)-DL-cysteine in D_2O + TFA-d_1.
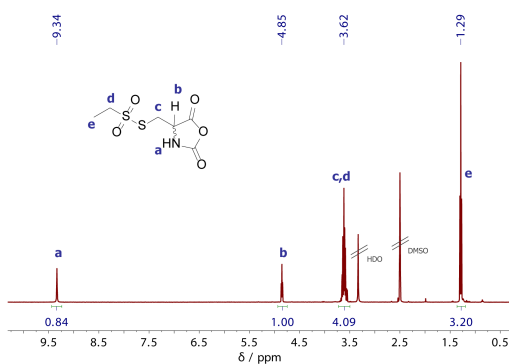
Figure S11. ^{1}H NMR spectrum of S-(ethylsulfonyl)-DL-cysteine N-carboxyanhydride in DMSO-d_6.
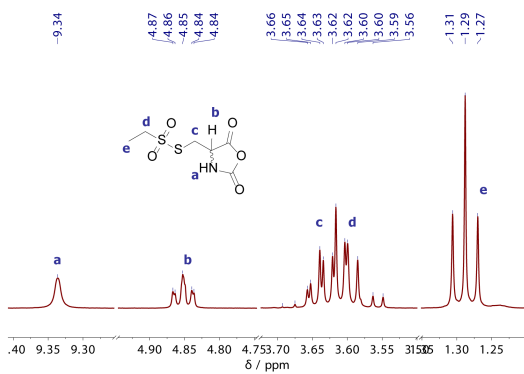
Figure S12. ¹H NMR spectrum of *S*-(ethylsulfonyl)-DL-cysteine *N*-carboxyanhydride in DMSO-*d₆*.
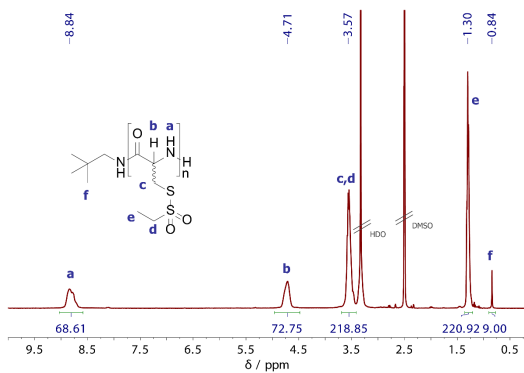
Figure S13. ¹H NMR spectrum of poly(*S*-(ethylsulfonyl)-DL-cysteine) in DMSO-*d₆*.
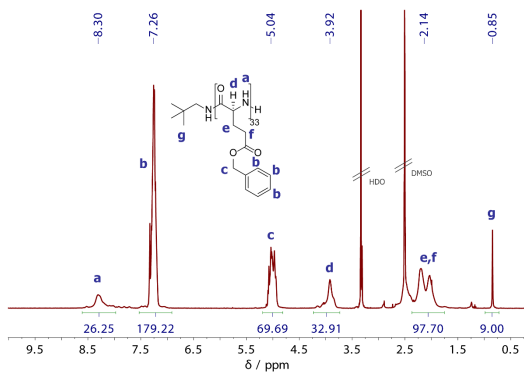
Figure S14. ¹H NMR spectrum of poly(ɣ-benzyl-L-glutamate) in DMSO-*d₆*.
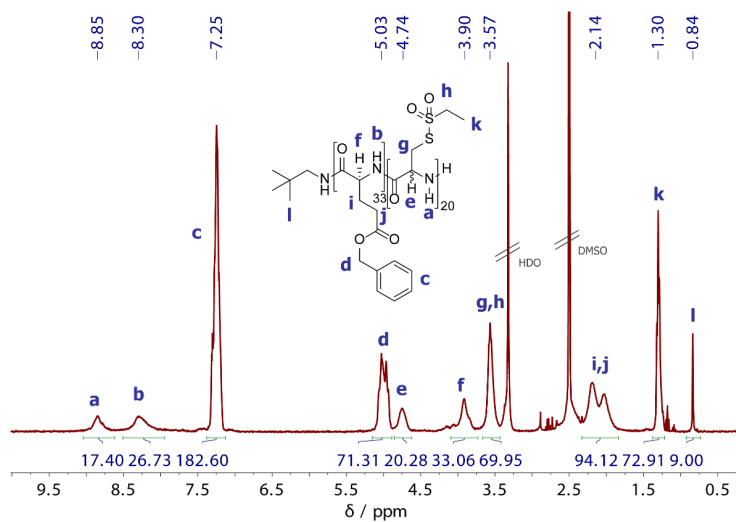
Figure S15. ^{1}H NMR spectrum of poly(γ-benzyl-L-glutamate)-*block*-poly(S-(ethylsulfonyl)-DL-cysteine) in DMSO-d_6.
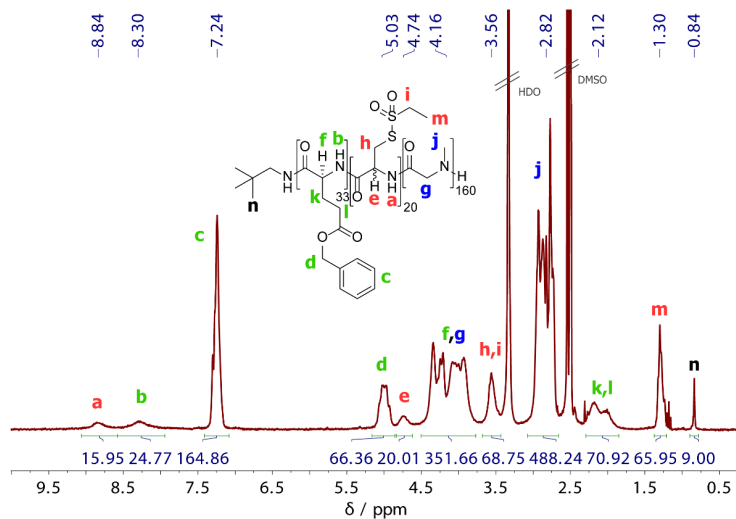

Figure S16. ^{1}H NMR spectrum of poly(γ-benzyl-L-glutamate)-*block*-poly(S-(ethylsulfonyl)-DL-cysteine)-*block*-poly(sarcosine) in DMSO-d_6.
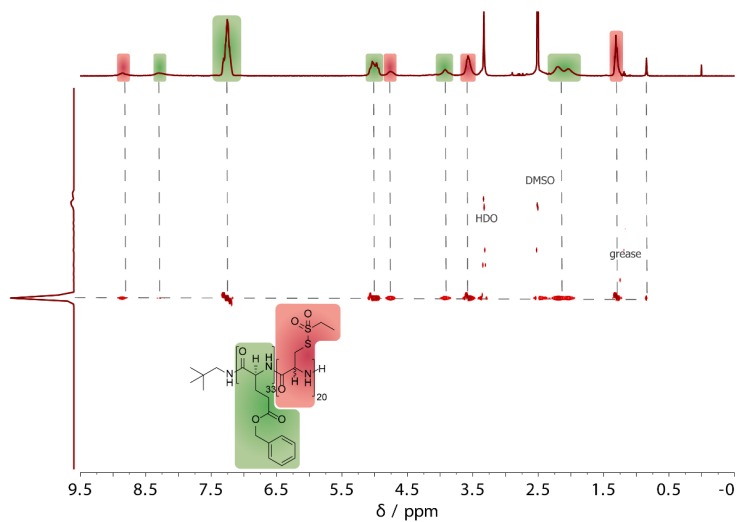
Figure S17. DOSY NMR spectrum of poly(γ-benzyl-L-glutamate)-*block*-poly(*S*-(ethylsulfonyl)-DL-cysteine) in DMSO-*d₆*.
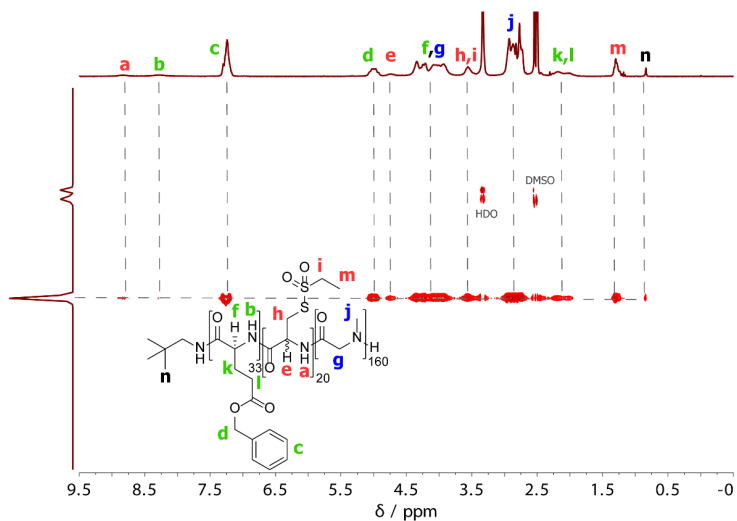

Figure S18. DOSY NMR spectrum of poly(γ-benzyl-L-glutamate)-*block*-poly(*S*-(ethylsulfonyl)-DL-cysteine)-*block*-poly(sarcosine) in DMSO-*d₆*.